

**Transverse-momentum distribution of ultrarelativistic protons in electromagnetic dissociation of  $^{32}\text{S}$  into  $p+^{31}\text{P}^*$** 

S. KAMEL

*Physics Department, Faculty of Education, Ain Shams University - Cairo, Egypt*

(ricevuto l' 1 Ottobre 1998; approvato il 29 Gennaio 1999)

**Summary.** — This work is devoted to study the transverse-momentum distribution of ultrarelativistic proton fragments in electromagnetic dissociation of  $^{32}\text{S}$  into  $p+^{31}\text{P}$  at 200 A GeV in nuclear emulsion. The experimental data have been compared with the predictions of Weizsacker-Williams (WW) theory and statistical theory of fragmentation. The transverse-momentum distribution of proton fragments is fitted by a double Rayleigh distribution having two different temperatures. The dependence of the parameters of this distribution on the incident projectile's mass number when compared with other experimental data, is investigated.

PACS 25.70 - Low and intermediate energy heavy-ion reactions.  
PACS 25.75 - Relativistic heavy-ion collisions.

**1. - Introduction**

Electromagnetic dissociation (EMD) study in the virtual photon field of the target nucleus [1] by the acceleration of heavy nuclei to relativistic energies offers an advantage over the experiments using photons on a fixed target. This advantage is that the reaction fragments are emitted with the same rapidity as the beam particles, so that they can be easily identified and measured. At relativistic energies, the statistical and non-statistical nature of the decay can be investigated to analyse the dynamics of Coulomb fragmentation, at least for studied projectile nuclei. In addition, heavy-ion reactions can be useful in measuring the excitation energy distribution which provides information about the electromagnetic excitation mechanism.

Few experiments have already been carried out to study the transverse-momentum ( $P_T$ ) distribution of relativistic proton projectile fragments (PFs) obtained either from nuclear collisions or EMD. For the former case, Ghosh *et al.* reported  $P_T$  distributions of relativistic proton PFs emerging from the interactions of two different projectiles with emulsion nuclei,  $^{12}\text{C}$  at 4.5 A GeV/c [2] and  $^{16}\text{O}$  at 60 A GeV/c [3], and compared the obtained distributions with Maxwell-Boltzmann distribution. Contrary to their expectations, which come out from the existence of two different types of events and two

(\* ) The author of this paper has agreed to not receive the proofs for correction.

different temperatures as was found in the case of relativistic  $\alpha$ -PFs, the two distributions of relativistic proton PFs reveal the evidence of a single temperature. This result is against Raha's proposal [4], which favours the existence of two different temperatures. Recently, El-Nadi *et al.* [5] support the expectation of having two different temperatures in the study of  $P_T$  distribution of relativistic proton PFs emerging from the interactions of  $^{32}\text{S}$ -emulsion at 3.7 A GeV.

Therefore, it is desirable to take up the present work with different mechanisms for better probing the dynamics of heavy-ion reactions. In this paper, the  $P_T$  distribution of proton emission via EMD of  $^{32}\text{S}$  beams at the highest available energy is studied using nuclear emulsion. Such detector, which covers a  $4\pi$  geometry, has a very high spatial resolution. This feature becomes very helpful especially at 200 A GeV, where the opening angles of PFs emitted in EMD events are very small ( $\sim 1$  mrad).

## 2. - Experimental details

In this experiment,  $^{32}\text{S}$  ions at 200 A GeV (CERN exp. No. EMU03) were used. Details of irradiation of the stack were given in ref. [6]. The pellicles were scanned by doubly scanning along the beam tracks, fast in the forward direction and slowly in the backward one. The beam tracks were picked up at a distance of 4 mm from the entrance edge, and within the central 80% of the pellicle thickness. With the use of the  $100\times$  magnification, each beam track was carefully followed up to a distance of 50 mm or until an interaction was observed. Since this study pertains to the pure EMD events, it is very important to

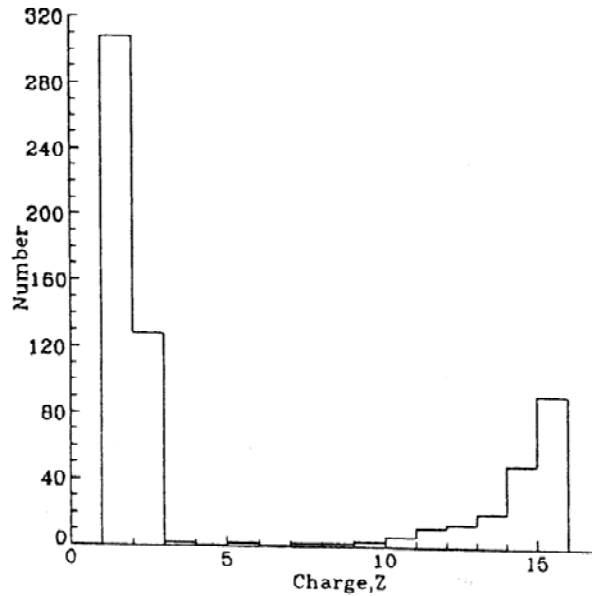


Fig. 1. - Charge spectrum of the PFs with  $1 \leq Z \leq 15$  emitted in EMD events for  $^{32}\text{S}$  at 200 A GeV.

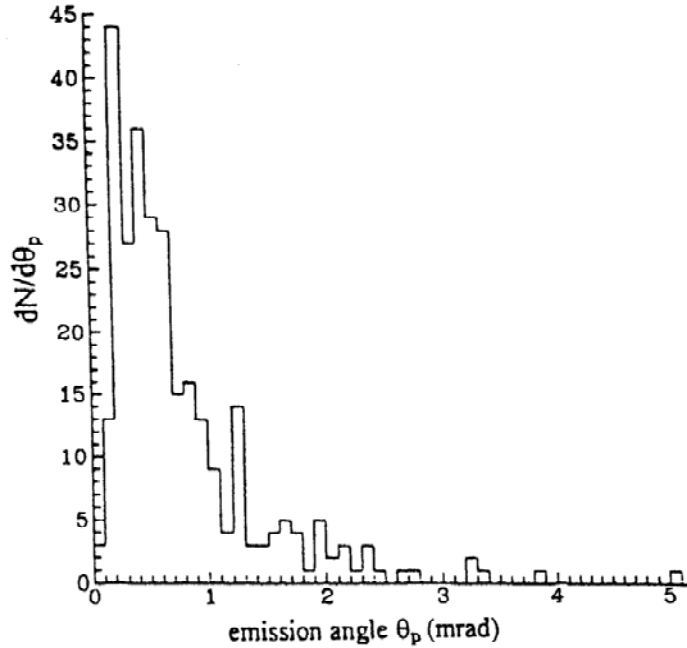


Fig. 2. - Angular distribution of  $Z = 1$  emitted in EMD of  $^{32}\text{S}$ .

candidate these events using the criteria [7] that

- a) all events show no target nuclear excitation ("black" and "grey" tracks) equal zero;
- b) the number of secondary produced particles (shower tracks) is zero;
- c) the sum of the measured charges of all outgoing fragments, produced with a narrow forward cone of  $\theta \leq \theta_c = 0.2/P_{\text{max}}$ , is always 16 for the  $^{32}\text{S}$  beam (where  $P_{\text{max}}$  stands for the beam momentum).

The charges of the PFs were determined by measuring the grain density and by  $\delta$ -ray counting following ref. [8]. Exclusion of low-energy  $e^+e^-$  pairs and high-energy  $\delta$ -rays was done [6,7]. The emission angles of all PFs in EMD events were determined from the vector directions of the incident beam and emitted fragments following ref. [8].

### 3. - Results

By applying the previous selection criteria, 210 EMD events were determined to be due to the clean breakup of the  $^{32}\text{S}$  projectile. Figure 1 shows the charge spectrum of all the PFs ranging from  $Z = 1$  to  $Z = 15$ . It is noticed that the most abundant PF is that with  $Z = 1$ , the next one is that with  $Z = 2$ . The ratio of PFs with  $Z = 1$  to those with  $Z = 2$  is almost 2.5. The PFs of charge  $Z = 15$  have a relative yield of almost 1.8 times those with  $Z = 14$ . These results for the 200 A GeV  $^{32}\text{S}$  beam are close to those of ref. [8]. Figure 2 shows the measured angular distribution for  $Z = 1$  PFs emitted in the total

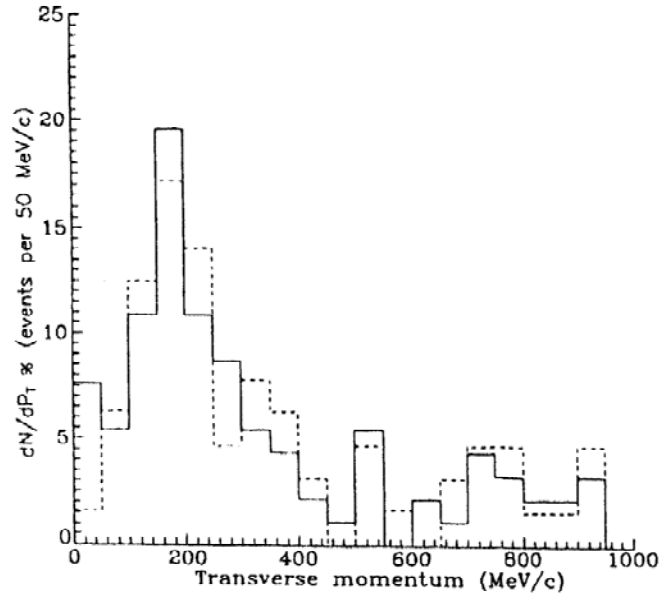


Fig. 3. -  $P_T$  distribution for protons in the decay mode  $^{32}\text{S}(\gamma, p)^{31}\text{P}$  (—, present work) together with the corresponding results of ref. [8] at 200 A GeV (- - -).

sample (210 EMD events) with an average emission angle  $\langle\theta_p\rangle = 0.889 \pm 0.081$  mrad. Table I displays the present relative rates of visible channels of a single proton and single alpha for EMD events compared with the corresponding results of refs. [7] and [8]. From this table it can be seen that the present emission of a single proton is about 3 times higher than that of a single alpha which is, within errors, in agreement with the corresponding results of ref. [8].

Since we are concerned with the relativistic protons in the breakup mode  $p+^{31}\text{P}$ , the details of the other various partial modes of decay of the  $^{32}\text{S}$  projectile at 200 A GeV are given elsewhere [9]. Accordingly, 92 events are collected to be the desired channel. From the measured values of the space angle  $\theta$ , the transverse momentum  $P_T$  of protons can be determined with the assumption that the projectile protons have the same longitudinal momenta as that of the incident  $^{32}\text{S}$  beam.

TABLE I. - Relative rates of visible channels of a single proton (1p) and single alpha (1 $\alpha$ ) emitted in EMD events of  $^{32}\text{S}$  at 200 A GeV.  $R$  is the ratio (1p)/(1 $\alpha$ ). The present work results are compared with the corresponding results of refs. [7] and [8].

Decay mode	Present work	Ref. [8]	Ref. [7]
single proton	$43.8 \pm 4.6$	$37.7 \pm 4.4$	$53.8 \pm 3.4$
single alpha	$14.3 \pm 2.6$	$13.1 \pm 2.6$	$6.0 \pm 1.0$
$R$	$3.1 \pm 0.5$	$2.9 \pm 0.8$	$8.9 \pm 3.6$

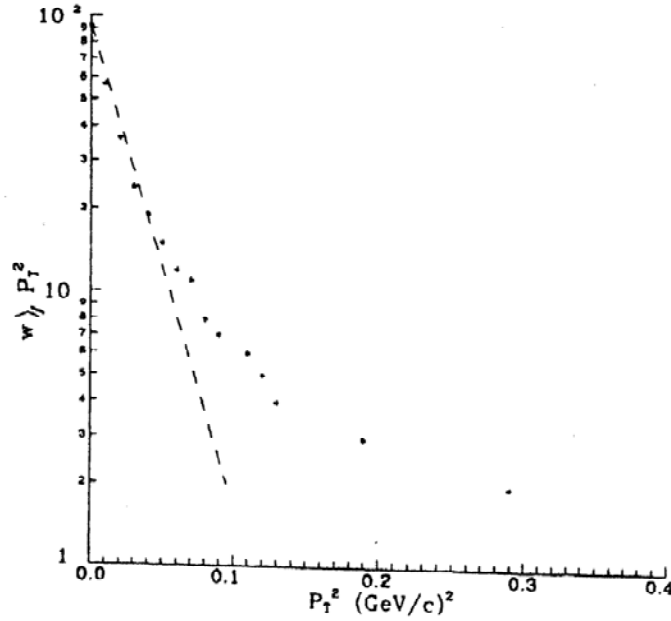


Fig. 4. - Integrated function  $W(\geq P_T^2)$  plotted against  $P_T^2$  for protons in the decay mode  $p+^{31}\text{P}$  at 200 A GeV  $^{32}\text{S}$  ions. The straight line is the corresponding distribution (1) with  $\sigma = \sigma_{\text{exp}}$ .

Figure 3 presents the  $P_T$  distribution of protons together with the corresponding distribution of ref. [8]. It can be seen that, within errors, the two distributions coincide. The peak of the present distribution corresponds to  $P_T = 199 \pm 18 \text{ MeV}/c$ . This value is in close agreement with that calculated according to WW theory [10], which gives [8]  $P_T = 190 \text{ MeV}/c$ . Consequently, the decay energy [11] ( $\Delta E_d$ ), defined as the energy transferred to the relativistic projectile from a stationary target in the EMD process, can be determined for the excitation of a resonant state. Therefore, from the measured value of  $P_T$  (199 MeV/c), the decay energy is calculated for the mode  $p+^{31}\text{P}$  using the relation  $\Delta E_d = P_T^2/2m_0$  (where  $m_0$  is the reduced mass of the used mode) and found to be 21 MeV. By comparing this value of the decay energy with that of the threshold energy [12] ( $\Delta E_{\text{th}} \approx 9 \text{ MeV}$ ), one can observe that the measured value of  $\Delta E_d$  is well above the excitation of the resonant state for the emission of a nucleon in the reaction  $^{32}\text{S} \rightarrow p+^{31}\text{P}$ . In this decay reaction, a great majority of events may be explained, following refs. [7-9], due to the absorption of giant dipole resonances (GDR).

Returning back to fig. 2, the angular distribution for the emission of a single proton in the total sample shows that few protons are emitted with angles greater than what is expected from pure projectile fragmentation. The proportion of the number of protons in the tail to that in the peak, deduced from the definition [13] of  $R_{\text{tp}}$ , equals 0.26, where

$$R_{\text{tp}} = \frac{\text{number of protons with } 1.1 < \theta_p \text{ (mrad)} \leq 5}{\text{number of protons with } \theta_p \text{ (mrad)} \leq 1.1}$$

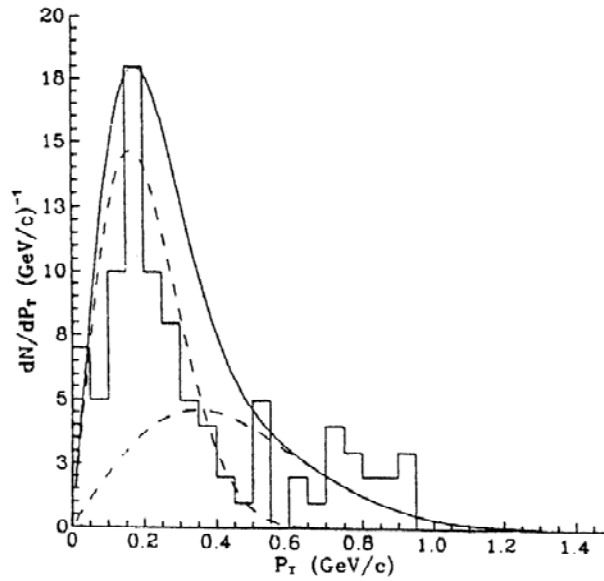


Fig. 5. - The approximation of the  $P_T$  distribution of protons in the reaction  $^{32}\text{S} \rightarrow \text{p} + ^{31}\text{P}$  at 200 A GeV by the double Rayleigh distribution (solid curve). The dashed curves are the contributions of the two parts of the distribution (2).

Figure 4 shows the distribution of  $P_T^2$  for the 92 relativistic protons emitted in the studied decay mode. This figure indicates that the  $P_T$  distribution of protons cannot be described by the single Rayleigh distribution [14]

$$(1) \quad f(P_T) = \left( \frac{P_T}{\sigma^2} \right) \exp \left[ \frac{-P_T^2}{2\sigma^2} \right], \quad \sigma = \sqrt{\frac{2}{\pi}} \langle P_T \rangle,$$

which is represented in the figure by the straight line. The  $P_T$  distribution of these proton fragments, which is shown in fig. 5, can be approximated by a double Rayleigh distribution characterized by two different dispersions (temperatures). The double Rayleigh distribution has the form [14]

$$(2) \quad F(P_T^2) = a \exp \left[ \frac{-P_T^2}{2\sigma_1^2} \right] + (1-a) \exp \left[ \frac{-P_T^2}{2\sigma_2^2} \right], \quad \sigma_{1,2} = \sqrt{\frac{2}{\pi}} \langle P_T \rangle_{1,2}, \quad \sigma_2 > \sigma_1$$

(where the third parameter  $a$  is the fraction of protons due to the main source at the lower temperature). In fig. 6, the double Rayleigh distribution is fitted to the data given in ref. [11] for the  $P_T$  distribution of protons in the  $^{16}\text{O} (\gamma, \text{p}) ^{15}\text{N}$  decay mode.

Table II shows, for each distribution, the experimentally obtained values of the average transverse momentum ( $\langle P_T \rangle$ ) and the values of the parameters of the double Rayleigh distribution. In this table, the fractions  $(1-a)$  of protons emitted by the secondary

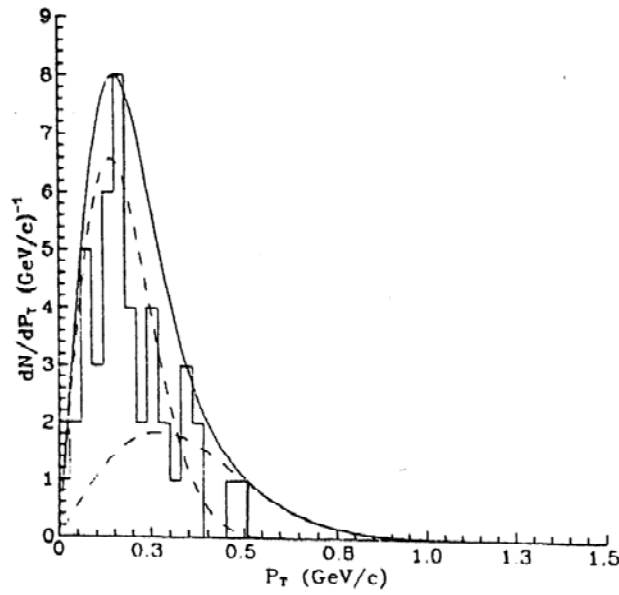


Fig. 6. - The fitting of the distribution (2) for protons in the  $^{16}\text{O}(\gamma, p)^{15}\text{N}$  decay mode for data given in ref. [11] at 200 A GeV.

high-temperature source, and the values of  $\chi^2/\text{DOF}$  are listed. Table II also displays the values of the corresponding parameters for the  $P_T$  distribution of protons ( $Z = 1$ ) PFs produced in the 3.7 A GeV  $^{32}\text{S}$ -Emulsion nuclear collisions [5]. From table II, it is noticed that the values of the parameters for the present work have somewhat increased with the incident projectile's mass number ( $A_p$ ). In addition, though the data of both mechanisms favour the existence of two parts of events, the so-called cold and hot events, the values of the parameters for the EMD are higher than the corresponding ones for the

TABLE II. - Average transverse momentum and values of parameters of the distribution (2) for protons produced in EMD events in two different projectiles at 200 A GeV, as well as the values of the corresponding parameters for proton PFs produced in the 3.7 A GeV  $^{32}\text{S}$ -emulsion nuclear collisions.

Projectile (A GeV)	Reaction	Experimental $\langle P_T \rangle_{\text{exp}}$ (GeV/c)	Parameters of double Rayleigh distribution				Ref.
			$\langle P_T \rangle_1$ (GeV/c)	$\langle P_T \rangle_2$ (GeV/c)	(1 - a)%	$\chi^2/\text{DOF}$	
$^{16}\text{O}$ (200)	EMD	$0.180 \pm 0.024$	0.175	0.338	35	1.070	[11]
$^{32}\text{S}$ (200)	EMD	$0.199 \pm 0.018$	0.207	0.439	40	0.704	Present work [5]
$^{32}\text{S}$ (3.7)	Nuclear	$0.169 \pm 0.007$	0.119	0.225	41	1.060	

nuclear collisions. This may be attributed to the different dynamic mechanisms and/or the increase of the incident projectile's energy.

#### 4. - Conclusion

From the data analysis, it may be concluded that

- 1) The emission of protons through the reaction  $^{32}\text{S}(\gamma, p)^{31}\text{P}$  at 200 A GeV is observed to be the dominant process ( $43.8 \pm 4.57\%$ ).
- 2) The excitation energy as determined from the measured value of  $P_T$  for the projectile protons in the decay mode  $^{32}\text{S} \rightarrow p + ^{31}\text{P}$  is well above the threshold energy for the formation of a resonant state. The majority of events in this mode may be attributed to the absorption of GDR [8,9].
- 3) The  $P_T$  distribution of proton fragments is peaked at a value in close agreement to that calculated according to WW theory.
- 4) The  $P_T$  distribution of proton fragments does not agree with that predicted by the statistical theory of fragmentation (single Rayleigh distribution). This is due to the presence of the non-statistical fragment excess with large values of  $P_T$ , such that the present distribution can be fitted by a double Rayleigh distribution having two different temperatures.
- 5) The temperatures and the fractions  $(1 - a)$  of non-statistical excess of proton fragments with high  $P_T$ -values show a reasonable dependence on  $A_p$ .
- 6) The present results may be supported by the findings of Barrete *et al.* [15] who reported the presence of a large non-statistical contribution in the decay mode  $^{28}\text{Si} \rightarrow p + ^{27}\text{Al}$ .

\* \* \*

This work was carried out at the High Energy Physics Laboratory, Faculty of Science, Cairo University. The author is deeply indebted to Prof. M. EL-NADI for his valuable comments and discussions. The author thanks his colleagues in the Emulsion Group for their help and also the authorities of CERN for irradiating the photographic plates.

#### REFERENCES

- [1] BERTULANI C. A. and BAUR G., *Phys. Rep.*, **163** (1988) 299.
- [2] GHOSH D. *et al.*, *Nuovo Cimento A*, **103** (1990) 423.
- [3] GHOSH D. *et al.*, *Nuovo Cimento A*, **110** (1997) 565.
- [4] RAHA S. *et al.*, *Phys. Rev. Lett.*, **53** (1984) 138.
- [5] EL-NADI M. *et al.*, *Radiat. Meas.*, **28** (1997) 231.
- [6] KAMEL S., *Phys. Lett. B*, **368** (1996) 291.
- [7] BARONI G. *et al.*, *Nucl. Phys. A*, **516** (1990) 673.
- [8] SINGH G. *et al.*, *Phys. Rev. C*, **41** (1990) 999.
- [9] HAFIZ M. E., Ph.D. thesis, Cairo University (1998); EL-NADI M. *et al.*, submitted for publication.
- [10] JACKSON J. D., *Classical Electrodynamics*, 2nd edition (Wiley, New York) 1975, p. 619.
- [11] SINGH G. and JAIN P. L., *Z. Phys. A*, **334** (1992) 73.
- [12] KAPLAN I., *Nuclear Physics*, 2nd edition (Benjamin, New York) 1962, p. 221.
- [13] BHALLA K. B. *et al.*, *Nucl. Phys. A*, **367** (1981) 446.
- [14] ABDURAZAKOVA U. A. *et al.*, *Sov. J. Nucl. Phys.*, **47** (1988) 827.
- [15] BARRETTE J. *et al.*, *Phys. Rev. C*, **41** (1990) 1512.